

Current-induced resonant motion of a magnetic vortex core: Effect of nonadiabatic spin torque

Jung-Hwan Moon,¹ Dong-Hyun Kim,² Myung Hwa Jung,³ and Kyung-Jin Lee^{1,*}
¹*Department of Materials Science and Engineering, Korea University, Seoul 136-701, Korea*
²*Department of Physics, Chungbuk National University, Cheongju 361-763, Korea*
³*Department of Physics, Sogang University, Seoul 121-742, Korea*

(Received 15 October 2008; revised manuscript received 2 February 2009; published 7 April 2009)

The current-induced resonant excitation of a magnetic vortex core is investigated by means of analytical and micromagnetic calculations. We find that the radius and phase shift of the resonant motion are not correctly described by the analytical equations because of the dynamic distortion of a vortex core. In contrast, the initial tilting angle of a vortex core is free from the distortion and determined by the nonadiabaticity of the spin torque. It is insensitive to experimentally uncontrollable current-induced in-plane Oersted field and thus allows a direct comparison with experimental results. We propose that a time-resolved imaging of the very initial trajectory of a core is a plausible way to experimentally estimate the nonadiabaticity.

DOI: 10.1103/PhysRevB.79.134410

PACS number(s): 75.70.Kw, 72.25.Ba, 85.75.-d

I. INTRODUCTION

A spin-polarized current can exert torque to a ferromagnet by transferring spin-angular momentum, i.e., spin-transfer torque. The spin-transfer torque provides full magnetization reversal, steady-state precession motion, and domain-wall movement.^{1,2} It is composed of adiabatic and nonadiabatic spin torque terms in continuously varying magnetization such as a magnetic domain wall. The adiabatic spin torque arises from the conduction electron spin whose projection on the film plane follows the direction of a local magnetization, whereas the nonadiabatic torque arises from a mismatch of the direction as a result of the momentum transfer or the spin relaxation.³⁻⁵

Until now, the experimental threshold current density J_C to steadily move a domain wall has been reported to be about 10^8 A/cm², too large for an application. In addition to the resonant depinning⁶ and the use of perpendicular anisotropy,⁷ an increase in β which is the ratio of the nonadiabatic spin torque to the adiabatic one can reduce J_C .⁸ Despite its importance, however, the exact value of β is still under debate even in theories;⁹⁻¹³ $\beta=0$, $\beta=\alpha$, and $\beta\neq\alpha$ where α is the Gilbert damping constant. This debate is also related to which mechanism between the Landau-Lifshitz damping and the Gilbert one is valid to describe the energy dissipation under the current injection.¹⁴ Experimental determination of β is essential to resolve this debate, but experimentally estimated values are also distributed; $\beta=8\alpha$,⁶ $\beta=\alpha$,¹⁵ $\beta>\alpha$,¹⁶ $\beta=2\alpha$,¹⁷ and $\beta\neq\alpha$.¹⁸ Since most experiments have used the same material (Permalloy), this wide distribution is caused by origins irrelevant to the material itself.

The wide distribution can originate from the Joule heating, the edge roughness of nanowire, and the in-plane component of the current-induced Oersted field H_{Oe}^{in} . The Joule heating significantly affects J_C and wall velocity.^{13,19} Therefore, it is difficult to precisely estimate β when the Joule heating is not negligible, i.e., $J_C > 10^8$ A/cm². In a magnetic nanowire, the edge roughness distorts and pins the domain wall²⁰ and thus prevents a proper interpretation of experimental data using theories derived for an ideal nanowire. A way to avoid the above issues is to experimentally study

resonant motions of a magnetic vortex core (VC) in a patterned disk by injecting an alternating current of the order of 10^7 A/cm². The magnetic vortex is an ideal system for the resonant motion study since VC can be considered as a topological point charge which efficiently responds to external forces.²¹⁻²³ It was experimentally confirmed that the VC can be resonantly excited by an ac current.^{6,17,24,25} Even in this case, however, a very small in-plane component of the ac-induced alternating Oersted field H_{Oe}^{in} inhibits a precise estimation of the spin torque parameters.^{25,26} Note that H_{Oe}^{in} is not a current-induced field along the thickness direction of the disk, but an in-plane field caused by any geometrical symmetry breaking of the system. The driving force due to H_{Oe}^{in} of only 0.3 Oe is as large as 30% of the total resonant excitation.²⁵ Such a small H_{Oe}^{in} is difficult to remove since it is caused by an uncontrollable nonuniform current distribution due to a geometrical symmetry breaking such as electric contacts or notches. Therefore, an experimental way to estimate the β which is safe from the Joule heating and the edge roughness and also insensitive to the H_{Oe}^{in} is highly desired.

In this work, we propose that a direct imaging of the very initial trajectory of VC induced by an ac is a plausible way to experimentally estimate β , which is free from all the three issues. We find that β does not change the resonant frequency but affects the phase of resonant motion. The phase shift is β dependent since β determines the tilting angle of the very initial trajectory measured from the direction of the electron flow. On the other hand, H_{Oe}^{in} with a typical magnitude does not change the tilting angle although it affects the steady resonant motion. We find that the initial tilting angle is only one physical observable which can be directly compared to the analytical result, whereas the others such as the radius and the phase shift are not correctly described by the analytical equations because of the dynamic distortion of VC.

This paper is organized as follows. After introducing theoretical approach (Sec. II) and micromagnetic simulation used in this work (Sec. III), we discuss the effect of β on the vortex dynamics (Sec. IV). In Sec. V, we summarize this work.

II. THEORETICAL FORMULAE OF THE VORTEX CORE DYNAMICS

The current-induced motion of VC is calculated using Thiele's equation with the spin-transfer torque terms [Eq. (1)],^{5,27-29}

$$\mathbf{G}(p) \times (\mathbf{u} - \dot{\mathbf{r}}) = -\frac{\delta U(\mathbf{r})}{\delta \mathbf{r}} - \alpha D \dot{\mathbf{r}} + \beta D \mathbf{u}, \quad (1)$$

where $G(p) = -G_0 p \mathbf{e}_z$ is the polarity ($p \pm 1$) dependent gyrovector, G_0 is obtained from the spin texture as

$$G_0 = \frac{M_S}{\gamma} \int dV \sin(\theta) (\vec{\nabla} \theta \times \vec{\nabla} \psi) \cdot \mathbf{e}_z, \quad (2)$$

$\theta(\psi)$ is the out-of-plane (in-plane) angle of the magnetization, M_S is the saturation magnetization, γ is the gyromagnetic ratio, $\mathbf{u} = u_0 \exp(i\omega t) \mathbf{e}_y$, $u_0 (= \mu_B J P / e M_S)$ is the amplitude of adiabatic spin torque, ω is the angular frequency of the ac, $\mathbf{r}(t) = X(t) + Y(t)$ is the time-dependent position vector of VC, and $U(r)$ is the potential well. The damping tensor D is also obtained from the integration of spin texture as

$$D = -\frac{M_S}{\gamma} \int dV [(\vec{\nabla} \theta \vec{\nabla} \theta + \sin^2(\theta) \vec{\nabla} \psi \vec{\nabla} \psi)]. \quad (3)$$

When VC is at the static equilibrium position, G_0 is $2\pi L M_S / \gamma$ and D is diagonal and $D_{xx} = D_{yy} = G_0 \ln(R/\delta)/2$ and $D_{zz} = 0$, where L is the thickness of disk, R is the vortex radius, and δ is the core diameter. Thiele's equation provides an analytical solution for the time-dependent position of VC when the VC does not change its shape in the dynamic motion. In other words, the potential profile U and all parameters such as G_0 and D should be assumed to be constant to obtain an analytical solution. We will discuss later whether or not this rigid VC assumption is valid.

With $X(t) = X_0 \exp(i\omega t)$, $Y(t) = Y_0 \exp(i\omega t)$, and $1 + (\alpha D / G_0)^2 \sim 1$, the solutions are in the form of $X(t) = X_1 \cos(\omega t) + iX_2 \sin(\omega t)$ and $Y(t) = Y_1 \cos(\omega t) + iY_2 \sin(\omega t)$ where

$$\begin{aligned} X_1 &= A p \omega_r [-(\omega_r^2 - \omega^2) + 2C^2 \alpha (\beta - \alpha) \omega^2], \\ X_2 &= A p \omega C [(\beta - \alpha) (\omega_r^2 - \omega^2) + 2\alpha \omega_r^2], \\ Y_1 &= A \omega_r C [\beta (\omega_r^2 - \omega^2) + 2\alpha (1 + C^2 \alpha \beta) \omega^2], \\ Y_2 &= A \omega [(1 + C^2 \alpha \beta) (\omega_r^2 - \omega^2) - 2C^2 \alpha \beta \omega_r^2]. \end{aligned} \quad (4)$$

Here, $A = u_0 / [(\omega_r^2 - \omega^2)^2 + (2C\alpha\omega_r\omega)^2]$, $\omega_r = \kappa / G_0$ is the resonance frequency, $\kappa = (dU/dr)/r$ is the effective stiffness coefficient of the potential well, and C is $D/G_0 = \ln(R/\delta)/2$. From Eq. (4), one finds the radius $a(t) = \sqrt{X(t)^2 + Y(t)^2}$, and the phase shift ϕ between the phase of the core gyration and that of the ac,

$$\begin{aligned} \phi &= \tan^{-1} \left(\frac{X_1}{Y_1} \right) \\ &= \tan^{-1} \left\{ \frac{1 - (\omega_r/\omega)^2 + 2C^2 \alpha (\beta - \alpha)}{C\beta [(\omega_r/\omega)^2 - 1] + 2C\alpha (1 + C^2 \alpha \beta)} \right\}. \end{aligned} \quad (5)$$

III. NUMERICAL MODEL

In order to check the validity of the analytical solutions, the micromagnetic simulation is also performed by means of the Landau-Lifshitz-Gilbert equation including the spin torque terms,

$$\begin{aligned} \frac{\partial \mathbf{M}}{\partial t} &= -\gamma \mathbf{M} \times \mathbf{H}_{\text{eff}} + \frac{\alpha}{M_S} \mathbf{M} \times \frac{\partial \mathbf{M}}{\partial t} + \mathbf{u} \cdot \nabla \mathbf{M} \\ &\quad - \frac{\beta}{M_S} [\mathbf{u} \cdot (\mathbf{M} \times \nabla) \mathbf{M}], \end{aligned} \quad (6)$$

where \mathbf{H}_{eff} is the effective field including the external, the magnetostatic, the exchange, and the current-induced Oersted field. The current-induced dynamics of the vortex core is micromagnetically modeled using a computational framework based on the fourth-order Runge-Kutta method. The model system is a circular Permalloy disk with the thickness of 10 nm and the diameter of 270 nm which is vortex-favored dimension [Fig. 1(a)]. The unit cell size is $2 \times 2 \times 10 \text{ nm}^3$ on a two-dimensional grid. The integration time step is 0.2 ps. The ac flows along the y axis and uniform current distribution is assumed through the disk. The maximum current density is $1.25 \times 10^7 \text{ A/cm}^2$. We did not take into account the Joule heating effect since it is negligible at this current density.³⁰ Standard material parameters for Permalloy are used: $M_S = 800 \text{ emu/cm}^3$, $\gamma = 1.76 \times 10^7 \text{ Oe}^{-1} \text{ s}^{-1}$, $\alpha = 0.01$, $P = 0.7$, and the exchange constant $A_{\text{ex}} = 1.3 \times 10^{-6} \text{ erg/cm}$.

IV. EFFECT OF β ON THE VORTEX CORE DYNAMICS

First, we assume $H_{\text{Oe}}^{\text{in}} = 0$ in order to investigate the effect originating exclusively from β on the resonant motion. We will recall the effect of $H_{\text{Oe}}^{\text{in}}$ in the last part. In Figs. 2(a) and 2(b), we show analytical and modeling results of the time averaged value $\langle Y(t) \cdot I_0 \sin(\omega t) \rangle / I_0$ at various β terms. To obtain analytical results, we use $C = 1.3$ because R is 135 nm and δ is 10 nm, determined from the micromagnetic configuration at the initial equilibrium state. $\langle Y(t) \cdot I_0 \sin(\omega t) \rangle / I_0$ shows a peak at the resonance frequency ω_r of 360 MHz. The peak structure is in general asymmetric regardless of β because the phase shift is dependent on the angular frequency ω [see Eq. (5) and Fig. 3(a)]. ω_r does not change with β whereas the peak structure becomes more asymmetric as β increases.

In spite of qualitative agreement, however, analytical results are quantitatively different from modeling ones. This is because the radius of gyroscopic motion is different between the modeling result and the analytic solution [inset of Fig. 2(b)]. We attribute this difference to a dynamic distortion of VC. As shown in Fig. 2(c), the VC shape in the initial equilibrium state is symmetric whereas it is asymmetric in a dynamic motion. The distortion changes the gyroscopic parameter G_0 , the damping tensor D (thus, the parameter C) and the effective stiffness coefficient κ since all parameters are determined by details of the spin texture [see Eqs. (2) and (3) and the definition of κ]. From micromagnetic spin textures of the vortex in the dynamic motion, we find that both C and κ

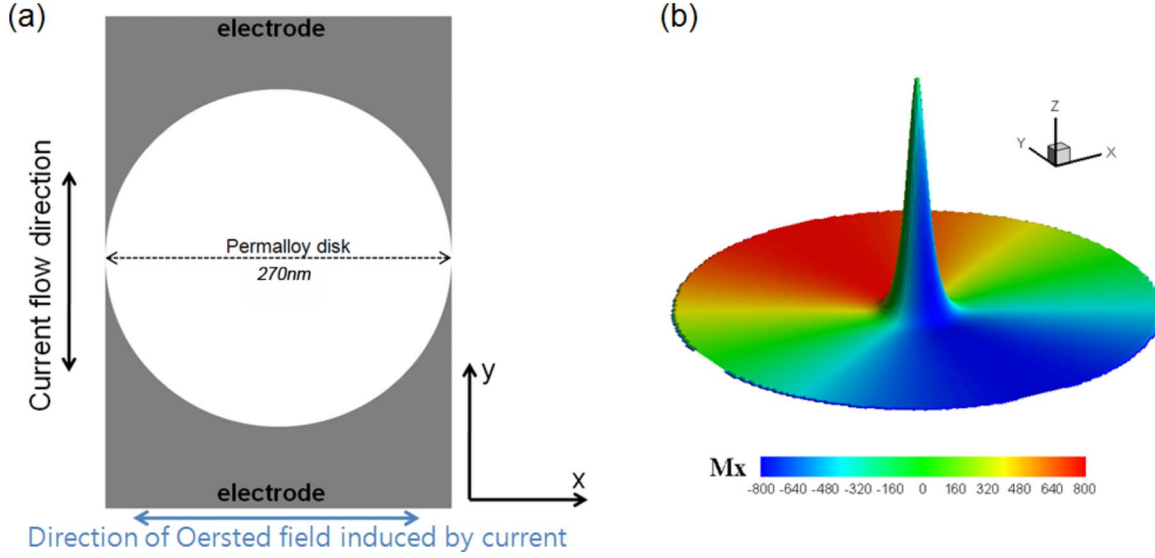


FIG. 1. (Color online) (a) Schematics of the model system. (b) Magnetization of a vortex in its initial equilibrium state. The height denotes the z component, whereas the color scale corresponds to the direction of the x component of magnetization.

increase from the initial equilibrium values because of the dynamic distortion [Fig. 2(d)]. The increase in κ is much larger than that of C , and responsible for the reduced radius in the modeling results because κ is directly connected to the resonance frequency in the theory. This increase in κ occurs at the very initial time stage, indicating that the assumption of the rigid VC and potential well is invalid except for the very initial trajectory. We have checked if Thiele's equation can reproduce the micromagnetic simulations with significantly better accuracy by considering some of the parameters of the equation as adjustable parameters (e.g., G_0 , D , and κ). However, we found that no parameter adjustment can reproduce. It indicates that Thiele's equation has a limitation to fully describe the long-time vortex dynamics due to its assumption of the fixed magnetic texture. Therefore, even when H_{Oe}^{in} is zero, it may be difficult to deduce important spin-torque parameters by directly comparing analytical solutions with experimental measurements of the steady gyroscopic motion.

Nevertheless, it is worthwhile investigating how β induces the additional asymmetry in the peak structure. Figure 3(a) shows analytical phase shifts at various β terms. As β increases, the absolute value of the phase shift ϕ decreases (increases) for the frequency smaller (higher) than ω_r . In other words, a vertical offset $\phi(\beta) - \phi(\beta = \alpha)$ of the phase shift increases with increasing β . From Eq. (4) with $\alpha \ll 1$ and $\beta \ll 1$, one can find that the vertical offset is approximately $\tan^{-1}[C(\beta - \alpha)]$ and thus dependent on β . This is why the peak structure becomes more asymmetric as β increases. However, quantitative disagreement between analytic solution and modeling result was again observed [inset of Fig. 3(a)]. The difference becomes larger as the radius of core gyration increases; i.e., the frequency approaches ω_r . This is also caused by the dynamic distortion of VC as explained above.

The vertical offset is β dependent since the initial tilting angle θ_{int} is determined by β [Fig. 3(b)]. VC initially moves along the direction of the electron flow. Because of the im-

balance of magnetostatic field, VC experiences the centripetal force and starts to undergo a gyration motion. In the absence of H_{Oe}^{in} , θ_{int} of the initial trajectory can be obtained from Eq. (1) by dropping the potential gradient term since VC is initially at the bottom of the potential well where the gradient is zero. When H_{Oe}^{in} is nonzero, the potential gradient is no longer zero and could affect θ_{int} . In order to investigate the effect of H_{Oe}^{in} on θ_{int} , we perform micromagnetic simulations for the initial trajectory with and without taking into account H_{Oe}^{in} . We assume that an alternating H_{Oe}^{in} is applied along the x axis and its magnitude is 0.3 Oe which is similar with the estimated value in the experiment in Ref. 25. As shown in Fig. 4(a), the effect of H_{Oe}^{in} on the very initial trajectory is negligible whereas the difference in trajectories between the two cases becomes larger and larger as the time evolves. This insensitivity of the initial trajectory and thus θ_{int} to H_{Oe}^{in} is valid for a different β (not shown). Thus, we drop the potential gradient term in Eq. (1) to derive θ_{int} . With $p = +1$ and the direction of the initial current along the $+y$ axis, one finds

$$\begin{aligned} \alpha D \dot{X} - G_0 \dot{Y} &= G_0 u_0, \\ G_0 \dot{X} + \alpha D \dot{Y} &= -\beta D u_0, \end{aligned} \quad (7)$$

where \dot{X} and \dot{Y} are the velocity along the x and y axes, respectively. By solving Eq. (7) for \dot{X} and \dot{Y} ,

$$\begin{aligned} \dot{X} &= G_0 u_0 D \frac{\alpha - \beta}{\alpha^2 D^2 + G_0^2}, \\ \dot{Y} &= -u_0 \frac{G_0^2 + \alpha \beta D^2}{\alpha^2 D^2 + G_0^2}. \end{aligned} \quad (8)$$

The initial tilting angle θ_{int} is given by

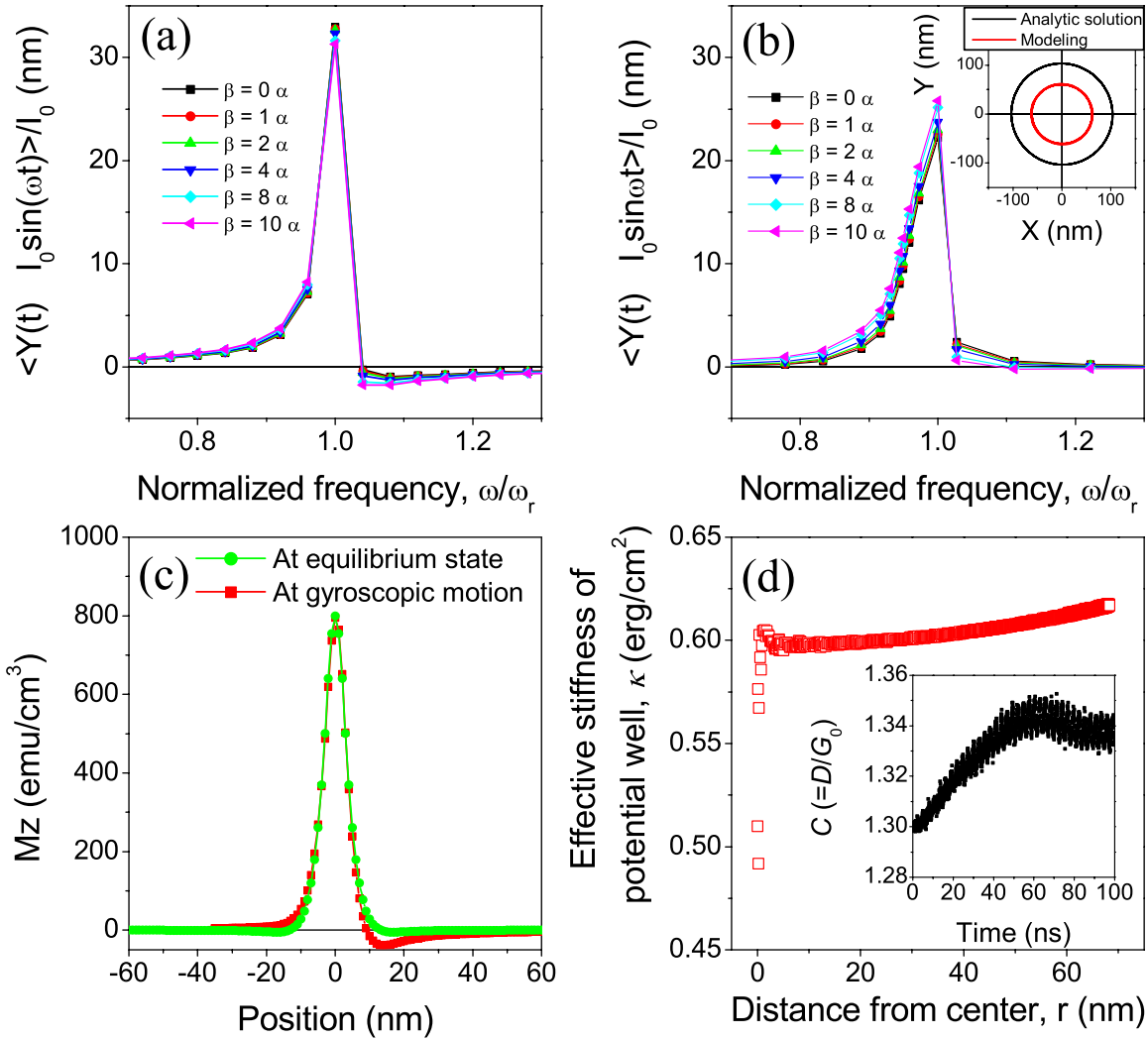


FIG. 2. (Color online) $\langle Y(t) \cdot I_0 \sin(\omega t) \rangle / I_0$ as a function of the frequency obtained from (a) analytic solution of Thiele’s equation and (b) micromagnetic simulation. (c) Comparison of the shape of vortex core, and (d) variation in κ as a function of the gyration radius. The inset of (b) shows the vortex core trajectories. The inset of (d) shows variation in the parameter $C(=D/G_0)$ with the time evolution. Both insets are obtained at $\beta=0$ and $\omega=\omega_r$.

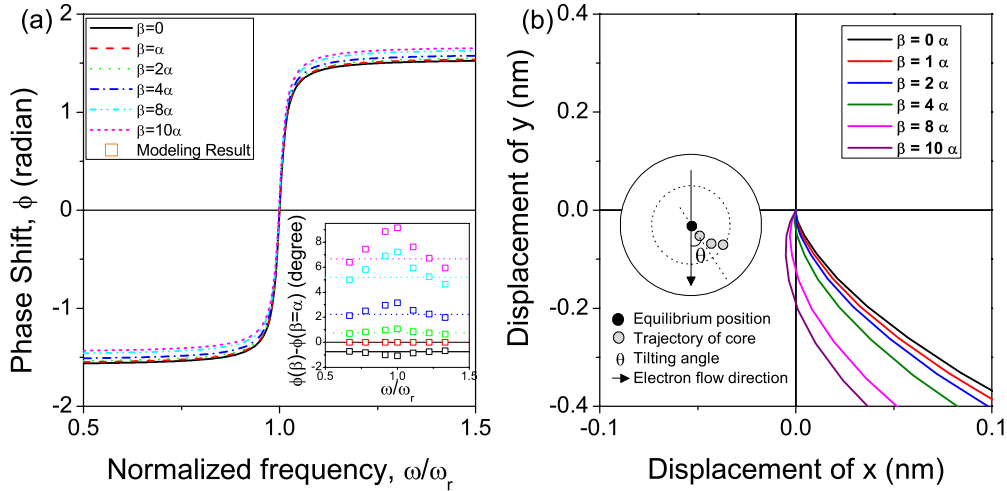


FIG. 3. (Color online) (a) Phase shift as a function of the frequency for various β terms. (b) Initial vortex core trajectories for various β terms ($\omega=\omega_r$). Inset of (a) shows the vertical offset of the phase shift for various β terms. In the inset, open symbols are obtained from micromagnetic modeling. Inset of (b) describes the definition of the initial tilting angle. The results were obtained at $H_{Oe}^{in}=0$.

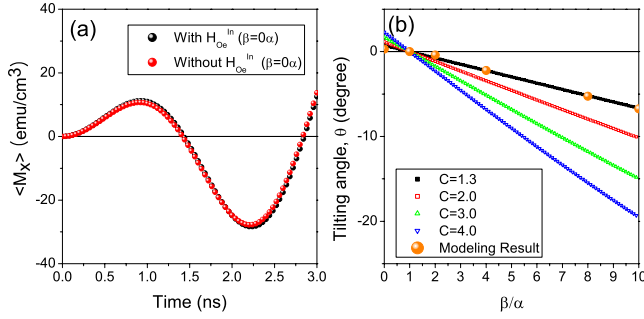


FIG. 4. (Color online) (a) Effect of in-plane Oersted field (H_{Oe}^{in}) on the initial trajectory of vortex core ($\beta=0$ and $\omega=\omega_r$), and (b) effect of β and C on the initial tilting angle.

$$\theta_{\text{int}} = \tan^{-1}\left(\frac{\dot{X}}{-\dot{Y}}\right) = \tan^{-1}\left(\frac{C(\alpha - \beta)}{1 + \alpha\beta C^2}\right). \quad (9)$$

Note that Eq. (9) is equivalent to the equation for the vertical phase shift with considering the sign of the initial ac and $\alpha\beta \ll 1$. It confirms that the vertical shift originates from the β -dependent θ_{int} . Figure 4(b) shows θ_{int} as a function of β/α for various values of C . It should be noted that θ_{int} 's obtained from modeling are in excellent agreement with analytical ones in contrast to the radius and phase shift. It is because VC retains its equilibrium shape at the very initial time stage where C and κ hardly change. It also confirms that dropping the potential gradient term is valid to derive the initial tilting angle.

For the Permalloy disk tested in this work ($C=1.3$), the difference in θ_{int} between $\beta=0$ and $\beta=10\alpha$ is about 7° which may be too small to experimentally measure. However, the β -dependent θ_{int} becomes larger as the parameter C increases. The C increases as the disk diameter increases. For

instance, the difference in θ_{int} between $\beta=0$ and $\beta=10\alpha$ is about 15° at $C=2.65$ corresponding to the disk diameter of $4 \mu\text{m}$ and the core diameter of 10 nm . The core diameter can be determined by micromagnetic calculation or magnetic force microscopy imaging for a given disk geometry.

Finally, we propose that a time-resolved magnetic imaging with high spatial resolution such as x-ray microscopy³¹ for observation of the very initial trajectory of VC in a wide disk is a possible way to experimentally estimate β . The x-ray imaging technique may not give a very accurate β because of its spatial resolution ($\approx 15 \text{ nm}$). However, it can allow us to estimate a possible range of β which is still useful for a better understanding of the nonadiabaticity of spin torque. Furthermore, it can at least differentiate whether or not β is larger than α . This is very important to understand the spin transport in domain walls since β larger than α is possible only when other mechanisms of momentum transfer exists in addition to the transfer of the spin-angular momentum from a spin-polarized current.¹⁶

V. SUMMARY

Using analytical and micromagnetic calculations, we investigate effects of the nonadiabatic spin torque on the resonant motion of a vortex core induced by an ac. We find that the initial trajectory of a vortex core is dependent on β and insensitive to an uncontrollable in-plane component of the current-induced Oersted field. A direct imaging of the very initial trajectory of a vortex core can be a way to experimentally determine β .

ACKNOWLEDGMENTS

This work was supported by a Korea Research Foundation Grant funded by the Korean Government (MOEHRD) (Grant No. KRF-2006-311-D00102).

*Corresponding author; kj_lee@korea.ac.kr

¹L. Berger, J. Appl. Phys. **55**, 1954 (1984); **71**, 2721 (1992).

²J. C. Slonczewski, J. Magn. Magn. Mater. **159**, L1 (1996).

³G. Tatara and H. Kohno, Phys. Rev. Lett. **92**, 086601 (2004).

⁴S. Zhang and Z. Li, Phys. Rev. Lett. **93**, 127204 (2004).

⁵A. Thiaville, Y. Nakatani, J. Miltat, and Y. Suzuki, Europhys. Lett. **69**, 990 (2005).

⁶L. Thomas, M. Hayashi, X. Jiang, R. Moriya, C. Rettner, and S. S. P. Parkin, Nature (London) **443**, 197 (2006).

⁷S.-W. Jung, W.-J. Kim, T.-D. Lee, K.-J. Lee, and H.-W. Lee, Appl. Phys. Lett. **92**, 202508 (2008).

⁸G. Tatara, T. Takayama, H. Kohno, J. Shibata, Y. Nakatani, and H. Fukuyama, J. Phys. Soc. Jpn. **75**, 064708 (2006).

⁹S. E. Barnes and S. Maekawa, Phys. Rev. Lett. **95**, 107204 (2005).

¹⁰Y. Tserkovnyak, H. J. Skadsem, A. Brataas, and G. E. W. Bauer, Phys. Rev. B **74**, 144405 (2006).

¹¹H. Kohno, G. Tatara, and J. Shibata, J. Phys. Soc. Jpn. **75**, 113706 (2006).

¹²J. Xiao, A. Zangwill, and M. D. Stiles, Phys. Rev. B **73**, 054428

(2006).

¹³S.-M. Seo, W.-J. Kim, T.-D. Lee, and K.-J. Lee, Appl. Phys. Lett. **90**, 252508 (2007).

¹⁴M. D. Stiles, W. M. Saslow, M. J. Donahue, and A. Zangwill, Phys. Rev. B **75**, 214423 (2007).

¹⁵M. Hayashi, L. Thomas, Y. B. Bazaliy, C. Rettner, R. Moriya, X. Jiang, and S. S. P. Parkin, Phys. Rev. Lett. **96**, 197207 (2006).

¹⁶M. Hayashi, L. Thomas, C. Rettner, R. Moriya, Y. B. Bazaliy, and S. S. P. Parkin, Phys. Rev. Lett. **98**, 037204 (2007).

¹⁷R. Moriya, L. Thomas, M. Hayashi, Y. B. Bazaliy, C. Rettner, and S. S. P. Parkin, Nat. Phys. **4**, 368 (2008).

¹⁸L. Heyne *et al.*, Phys. Rev. Lett. **100**, 066603 (2008).

¹⁹E. Martinez, L. Lopez-Diaz, O. Alejos, L. Torres, and C. Tristan, Phys. Rev. Lett. **98**, 267202 (2007).

²⁰J. He, Z. Li, and S. Zhang, J. Appl. Phys. **99**, 08G509 (2006).

²¹K. Yu. Guslienko, B. A. Ivanov, V. Novosad, Y. Otani, H. Shima, and K. Fukamichi, J. Appl. Phys. **91**, 8037 (2002).

²²S.-K. Kim, Y.-S. Choi, K.-S. Lee, K. Yu. Guslienko, and D.-E. Jeong, Appl. Phys. Lett. **91**, 082506 (2007).

²³J.-H. Moon, W.-J. Kim, T.-D. Lee, and K.-J. Lee, Phys. Status

- Solidi B **244**, 4491 (2007)
- ²⁴S. Kasai, Y. Nakatani, K. Kobayashi, H. Kohno, and T. Ono, Phys. Rev. Lett. **97**, 107204 (2006).
- ²⁵M. Bolte *et al.*, Phys. Rev. Lett. **100**, 176601 (2008).
- ²⁶B. Krüger, A. Drews, M. Bolte, U. Merkt, D. Pfannkuche, and G. Meier, Phys. Rev. B **76**, 224426 (2007).
- ²⁷A. A. Thiele, Phys. Rev. Lett. **30**, 230 (1973).
- ²⁸J. Shibata, Y. Nakatani, G. Tatara, H. Kohno, and Y. Otani, Phys. Rev. B **73**, 020403(R) (2006).
- ²⁹J. He, Z. Li, and S. Zhang, Phys. Rev. B **73**, 184408 (2006).
- ³⁰C.-Y. You, I. M. Sung, and B.-K. Joe, Appl. Phys. Lett. **89**, 222513 (2006).
- ³¹P. Fischer, D.-H. Kim, W. Chao, J. A. Liddle, E. H. Anderson, and D. T. Attwood, Mater. Today **9**, 26 (2006).